



OPEN ACCESS

EDITED BY

Hongliang Dai,
Jinzhou Medical University, China

REVIEWED BY

Zaid Altaany,
Yarmouk University, Jordan
Qi Guo,
Hebei Medical University, China

*CORRESPONDENCE

Han Li,
✉ hanli@ccmu.edu.cn

SPECIALTY SECTION

This article was submitted to
Cardiovascular and Smooth Muscle
Pharmacology,
a section of the journal
Frontiers in Pharmacology

RECEIVED 25 August 2022

ACCEPTED 29 November 2022

PUBLISHED 15 December 2022

CITATION

Feng J, Li H and Wang S (2022),
Hydrogen sulfide alleviates uremic
cardiomyopathy by regulating PI3K/
PKB/mTOR-mediated overactive
autophagy in 5/6 nephrectomy mice.
Front. Pharmacol. 13:1027597.
doi: 10.3389/fphar.2022.1027597

COPYRIGHT

© 2022 Feng, Li and Wang. This is an
open-access article distributed under
the terms of the [Creative Commons
Attribution License \(CC BY\)](https://creativecommons.org/licenses/by/4.0/). The use,
distribution or reproduction in other
forums is permitted, provided the
original author(s) and the copyright
owner(s) are credited and that the
original publication in this journal is
cited, in accordance with accepted
academic practice. No use, distribution
or reproduction is permitted which does
not comply with these terms.

Hydrogen sulfide alleviates uremic cardiomyopathy by regulating PI3K/PKB/mTOR-mediated overactive autophagy in 5/6 nephrectomy mice

Jianan Feng, Han Li* and Shixiang Wang

Department of Nephrology, Beijing Chao-Yang Hospital, Capital Medical University, Beijing, China

The gasotransmitter hydrogen sulfide (H₂S) plays important physiological and pathological roles in the cardiovascular system. However, the involvement of H₂S in recovery from uremic cardiomyopathy (UCM) remains unclear. This study aimed to determine the therapeutic efficacy and elucidate the underlying mechanisms of H₂S in UCM. A UCM model was established by 5/6 nephrectomy in 10-week-old C57BL/6 mice. Mice were treated with sodium hydrosulfide (NaHS, H₂S donor), L-cysteine [L-Cys, cystathionine gamma-lyase (CSE) substrate], and propargylglycine (PPG, CSE inhibitor). Treatment of H9C2 cardiomyocytes utilized different concentrations of uremic serum, NaHS, PPG, and PI3K inhibitors (LY294002). Mouse heart function was assessed by echocardiography. Pathological changes in mouse myocardial tissue were identified using hematoxylin and eosin and Masson's trichrome staining. Cell viability was assessed using the Cell Counting Kit-8. The protein expressions of CSE, p-PI3K, PI3K, p-PKB, PKB, p-mTOR, mTOR, and autophagy-related markers (Beclin-1, P62, and LC3) were detected using Western blotting. We found that NaHS and L-Cys treatment attenuated myocardial disarray, fibrosis, and left ventricular dysfunction in UCM mice. These abnormalities were further aggravated by PPG supplementation. Enhanced autophagy and decreased phosphorylation of PI3K, PKB, and mTOR protein expression by UCM were altered by NaHS and L-Cys treatment. *In vitro*, uremic serum increased overactive autophagy and decreased the phosphorylation levels of PI3K, PKB, and mTOR in cardiomyocytes, which was substantially exacerbated by endogenous H₂S deficiency and attenuated by pre-treatment with 100 μm NaHS. However, the protective effects of NaHS were completely inhibited by LY294002. These findings support a protective effect of H₂S exerted against UCM by reducing overactive autophagy through activation of the PI3K/PKB/mTOR pathway.

KEYWORDS

uremic cardiomyopathy, hydrogen sulfide, cardiomyocytes, autophagy, PI3K/PKB/mTOR signal

1 Introduction

Uremic cardiomyopathy (UCM) is a common complication in patients with chronic kidney disease (CKD), especially dialysis patients, which is associated with high mortality (Amador-Martínez et al., 2021). The characteristic pathological changes of UCM are left ventricular hypertrophy (LVH) and diastolic dysfunction in heart failure with preserved ejection fraction (HFpEF) phase. Subsequently, ventricular interstitial fibrosis, capillary thinning, and systolic dysfunction occur in heart failure with reduced ejection fraction (HFrEF) phase (Husain-Syed et al., 2015; Powers et al., 2016; Wang et al., 2017; Sárközy et al., 2018). The pathogenesis of UCM is multifactorial and complicated, involving hypertension, volume overload, activation of the renin-angiotensin-aldosterone system, stimulation of the β -adrenergic system, and insulin resistance. In addition, some specific factors that arise in uremia also play an important role, such as hyperparathyroidism, hyperphosphatemia, 1,25-dihydroxy-vitamin D deficiency, increased production of fibroblast growth factor 23, Klotho deficiency, circulating uremic toxins, and increases in endogenous cardiotonic steroid concentration (Vanholder et al., 2014; Spoto et al., 2016; Hung et al., 2017; Wang and Shapiro, 2019; Memmos and Papagianni, 2021).

Autophagy is a process that devours cytoplasmic proteins or organelles, entraps them into vesicles, and fuses them with lysosomes to form autophagic lysosomes that degrade the contents they entrap. Studies have shown that autophagy can scavenge waste within the cardiac system to achieve cellular homeostasis and organelle renewal (Wu et al., 2019). Under baseline conditions, autophagy plays a protective role in the structure and function of the heart, and can be activated under pressure to limit the aggravation of injury (Sciarretta et al., 2018). However, excessive and sustained activation of autophagy may cause heart damage under certain stress conditions such as reperfusion injury, starvation, diabetes, hypertension, and ischemia (Sciarretta et al., 2018; Shi et al., 2021). In pathological conditions, to fight the stress response, the heart will exhibit unrestrained autophagic activity, which promotes maladaptive cardiac remodeling and contributes to the development of cardiomyopathy (Porrello and Delbridge, 2009; Mei et al., 2015). However, the role of autophagy in UCM and the specific mechanisms involved are still unclear.

Hydrogen sulfide (H_2S) is a gasotransmitter that is endogenously produced in the cardiovascular system by cystathionine gamma-lyase (CSE), which has shown great potential in treating cardiovascular diseases (CVDs) (Kolluru et al., 2015). There is increasing evidence that H_2S regulates vascular tone and myocardial function in association with altered

autophagy (Zhang et al., 2018; LaPenna et al., 2021). Studies have demonstrated that the protective effect of H_2S against diabetes-induced myocardial fibrosis may be associated with attenuation of autophagy (Xiao et al., 2016). In smoking-induced cardiomyopathy, H_2S administration can decrease autophagy (Zhou et al., 2014). However, the effects of H_2S on UCM and its related mechanisms are still unknown.

Available evidence has demonstrated that mTOR activation is regulated by PI3K/PKB pathway activation, leading to inhibition of excessive autophagy and protection from cardiac hypertrophy (Kishore et al., 2015; Cheng et al., 2017). Thus, we hypothesized that H_2S protects against UCM *via* regulation of PI3K/PKB/mTOR-mediated autophagy. This study designed and conducted a series of *in vitro* and *in vivo* experiments to verify this hypothesis.

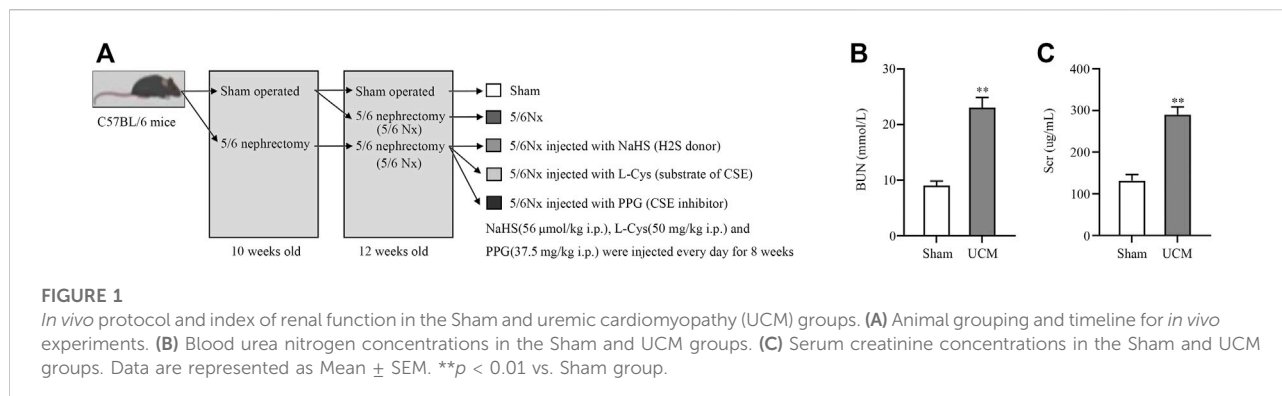
2 Materials and methods

2.1 Animals

C57BL/6 mice aged 9 weeks were purchased from Beijing Vital River Laboratory Animal Technology Co., Ltd (License No. SCXK, 2016-0006, Beijing) and were fed adaptively for 1 week. Animals were housed in a clean degree laboratory with three mice per cage, under a controlled temperature of 24°C, relative humidity of 35–50%, with free access to food and water.

2.2 Mouse model of 5/6 nephrectomy-induced UCM, drug administration and experimental groups

Under isoflurane anesthesia, the mouse model of 5/6 nephrectomy was performed as previously described (Leelahavanichkul et al., 2010). In brief, a longitudinal incision of approximately 1 cm was made on the lateral skin below the angle of the left costal ridge in mouse. Subsequently, the muscle was cut layer by layer, the left kidney was exposed, the renal capsule was separated, and 2/3 of the upper and lower pole renal tissue of the left kidney was removed, and then a gelatin sponge was used to compress and stop bleeding. One week later, the right kidney was exposed in the same way and the pedicle was ligated with 3-0 non-absorbable sutures. The right kidney was removed after ligation. In the Sham group, the skin was cut under anesthesia to separate the renal capsule, but the kidney was not resected. Eight weeks after the operation, obvious renal dysfunction was observed in UCM mice (Figures 1B, C,) using serum biochemistry, as described in Section 2.3 below.



Male C57BL/6J mice were fed with normal chow diet and randomly divided into five groups ($n = 6$ per group): Sham, UCM, UCM + NaHS, UCM + L-cys, and UCM + PPG. The Sham group mice had a renal capsule isolated without kidney damage. The UCM group mice underwent 5/6 nephrectomy. The UCM + NaHS group mice had UCM and were intraperitoneally injected with NaHS (H₂S donor, 56 μ mol/kg body weight/day). The UCM + L-cys group mice had UCM and were intraperitoneally injected with L-cys (substrate of CSE, 50 mg/kg body weight/day). The UCM + PPG group mice had UCM and were intraperitoneally injected with PPG (CSE inhibitor, 37.5 mg/kg body weight/day) (Figure 1A). All procedures were performed in accordance with the guidelines set by the recommendations of the Guide for the Care and Use of Laboratory Animals of the National Institutes of Health and approved by the Experimental Animal Ethics Committee of Beijing Chao-Yang Hospital, Capital Medical University.

2.3 Measurement of serum creatinine and blood urea nitrogen

Mice were fasted for at least 8 h before blood was collected in anticoagulant tubes. Serum creatinine and blood urea nitrogen were measured using the sarcosine oxidase method (Solarbio, BC4910, Beijing, China) and visible spectrophotometry (Solarbio, BC1530, Beijing, China) respectively, according to the manufacturer's protocol.

2.4 Measurement of H₂S concentration

H₂S concentrations in the plasma of all mice were measured using the zinc acetate reaction. The fresh blood was centrifuged at 500 g for 5 min, the plasma was immediately obtained, and rapidly added to the assay mixture. First, 100 μ L of plasma was added into a test tube containing distilled water and 1% zinc acetate; thereafter, N, N-dimethyl-p-phenylenediamine dihydrochloride in 7.2 M HCl and FeCl₃ in 1.2 M HCl were added. This mixture was incubated at room temperature for 20 min, after which 1 ml of 10% trichloroacetic acid

was added to the solution and centrifuged at 4,000 g for 10 min. The optical absorbance of the supernatant was measured with a spectrometer at 670 nm. All samples were assayed repeatedly, and the H₂S concentration in the solution was calculated against the calibration curve of the standard NaHS solution.

H₂S concentrations in H9C2 cardiomyocytes were measured using the micro-method (Solarbio, BC 2055, Beijing, China), according to the manufacturer's protocol.

2.5 Histopathology

Fresh mouse heart tissue was fixed in 4% paraformaldehyde solution, embedded in paraffin, and then cut into 4 μ m thick slices. The cut slices were dewaxed in xylene, with degraded alcohol hydration. The slides were stained with hematoxylin and eosin (H&E) or Masson's trichrome (Servicebio, G1005, Wuhan, China) according to the instructions.

For H&E staining, the degree of myocardial injury was scored according to the following criteria: 0, myocardial structure intact without injury; 1, mild myocardial interstitial edema and local necrosis; 2, extensive myocardial and interstitial edema accompanied by local medial necrosis; 3, severe small vessel injury and extensive myocardial necrosis, with a large number of inflammatory cell infiltrations and contraction band formation; and 4, severe diffuse myocardial necrosis and hemorrhage, massive small vessel injury, and formation of contraction band.

For Masson's trichrome staining results, collagen fibers were blue. The volume fraction of collagen was calculated as the ratio of positive collagen blue area to the whole tissue area.

2.6 Electrocardiogram measurements

A high-frequency ultrasound device (Vevo 2100, VisualSonics, Toronto, Canada) was utilized for ultrasound imaging. During this process, mice were anesthetized with 2–3% isoflurane in the induction chamber and maintained by inhalation of 1.0–1.5% isoflurane with 100% oxygen mask.

Measures across three cardiac cycles were averaged for all electrocardiogram measurements.

Measures from the left ventricle (LV) mid-papillary level in the parasternal long-axis view were conducted with 2D M-mode imaging, for: interventricular septum thicknesses at end-diastole and end-systole (IVSd and IVSs, respectively); LV internal diameters at end-diastole and end-systole (LVIDd, LVIDs); LV posterior wall thicknesses at end-diastole and end-systole (LVPWd and LVPWs); and stroke volume (SV), which was derived by the formula: $EDV - ESV$,

Where EDV and ESV are the end-diastolic and end-systolic volumes, respectively. LV systolic function was estimated by the ejection fraction (EF) derived from the formula: SV/EDV .

The area-length method (Zhang T. Y. et al., 2021) was used to calculate the LV mass, which was derived using the following formula: $LV \text{ mass, g} = 1.053 [(LVIDd + IVSd + LVPWd)^3 - (LVIDd)^3]$; $LV \text{ mass (corrected), g} = 0.8 \times LV \text{ mass}$.

Doppler measurements of mitral valve inflow velocities were recorded from an apical four-chamber view, with a cursor positioned at the tips of the mitral valve leaflets. Diastolic function was evaluated from measurements of early filling velocity (E), atrial filling velocity (A), and calculation of the ratio of the early to late diastolic mitral inflow velocities (E/A).

2.7 Cell culture and treatment and RNA infection

A sample of H9C2 cardiomyocytes was obtained from the China Cell Bank. These were cultured in Dulbecco's modified Eagle's medium (DMEM, 11966025, Gibco, NY 14072, United States) containing 10% (v/v) fetal bovine serum (FBS, 10099-141, Gibco, Grand Island, NY 14072, United States) and 1% (v/v) penicillin-streptomycin solution (15070063, Life Technologies, Carlsbad, Ontario, Canada) at 37°C in an incubator (MCO-5AC, Panasonic, Kyoto, Japan) with 5% CO₂.

H9C2 cardiomyocytes were transiently transfected with CSE-specific siRNA (Beijing likely biotechnology, Beijing, China) using lipofectamine 2000 (Thermo Fisher Scientific, Waltham, United States), and the cells were subsequently cultured for 48 h.

2.8 Human blood sampling

Human serum samples were taken to stimulate H9C2 cardiomyocytes *in vitro*. These samples were collected from four healthy participants and nine patients with end-stage renal failure who underwent hemodialysis. Serum was collected before the start of the hemodialysis session. The mean age of the healthy participants was 58.50 ± 7.05 years, and none had a family history

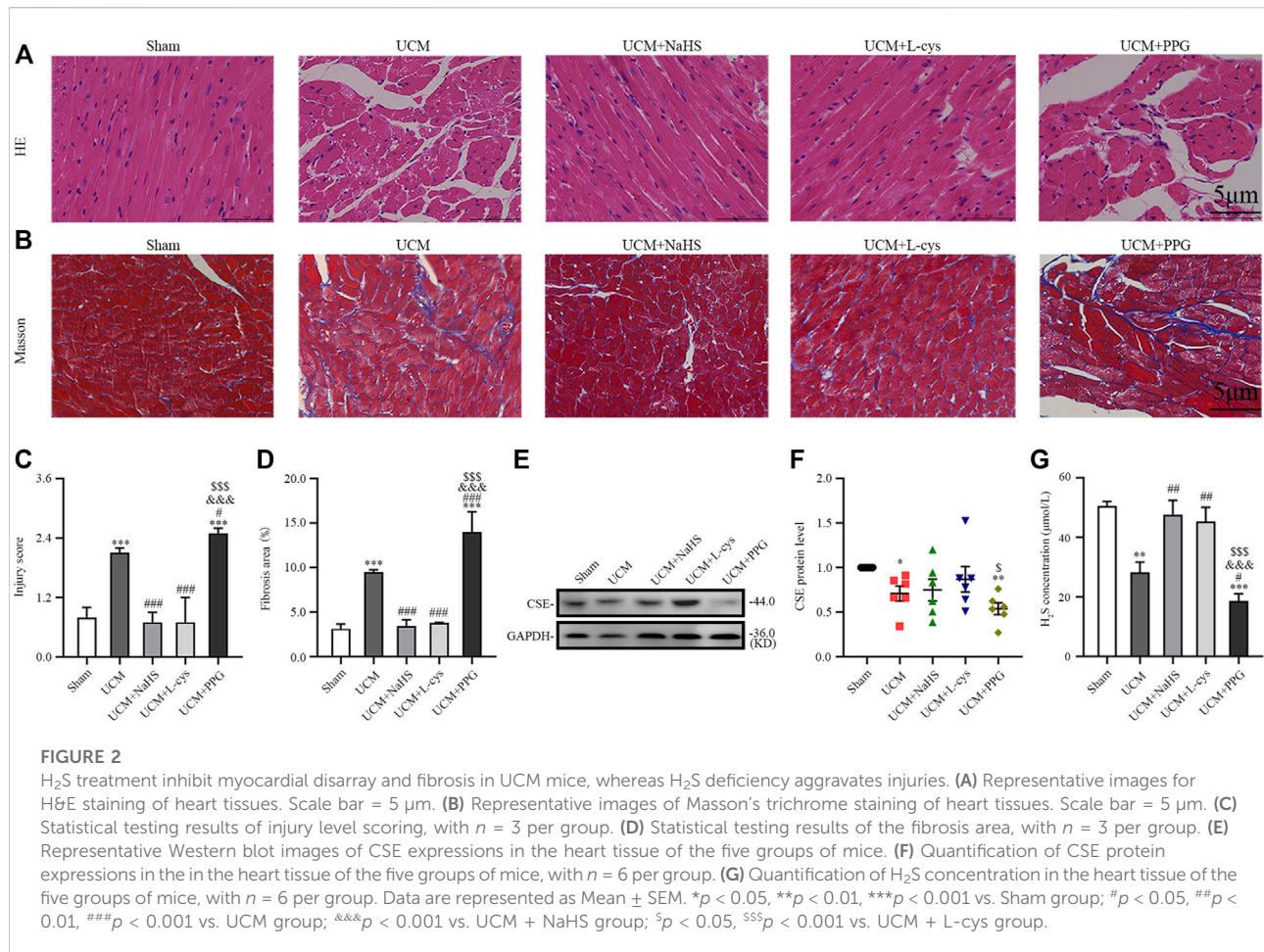
of diabetes, cardiovascular disease, or serious liver or kidney disease. The mean age of the hemodialysis patients was 58.89 ± 8.91 years, while the mean duration of hemodialysis therapy was 220.78 ± 31.46 months. Color doppler echocardiography was used to investigate enlargement of the heart. The study was conducted in accordance with the Declaration of Helsinki and approved by the Ethics Committee of Beijing Chao-Yang Hospital, Capital Medical University. Written informed consent was obtained from all participants.

2.9 Detection of cell viability

Cell Counting Kit-8 (CCK-8) assay (C0038, Beyotime Biotechnology, Shanghai, China) was used to assess H9C2 cell viability. Briefly, cells were cultivated in 96-well plates (2000 cells/well) and exposed to different concentrations of uremic serum and 25–200 μM NaHS in 10% uremic serum for 24 h. Then, 10 μL of the kit solution was mixed into the culture medium for 1 h. Absorbance was measured at 450 nm using a microplate reader (PerkinElmer EnSpire, MA, United States). Cell viability was expressed as a percentage of the control.

2.10 Western immunoblotting analysis

Mouse heart tissues and H9C2 cardiomyocytes were homogenized and thawed in radioimmunoprecipitation assay buffer (C1053, Applygen, Beijing, China) with protease inhibitors (04693116001, Roche, United States) and phosphatase inhibitors (04906837001). The protein concentration was determined using a BCA Protein Assay kit (23225; Pierce Company, Rockford, IL, United States). The samples were subjected to sodium dodecyl-sulfate polyacrylamide gel electrophoresis (SDS-PAGE) and subsequently transferred onto a polyvinylidene difluoride membrane (GE Healthcare, Buckinghamshire, United Kingdom). The membranes were blocked with 10% milk and incubated with primary antibodies at 4°C overnight. The primary antibodies used were CSE (1:1000, 12217-1-AP) and P62 (1:1000, 18420-1-AP) from Proteintech (Rosemont, IL 60018, United States); LC3 A/B (1:1000, 12741), P-p85 (Tyr458)/p55 (Tyr199)-PI3K (1:1,000, 4,228), PI3K (1:1,000, 4,257), P-Ser473-PKB (1:1,000, 4,060), PKB (1:1,000, 9272), mammalian target of rapamycin (mTOR, 1:1,000, 2983), P-Ser2448-mTOR (1:1,000, 5536) from Cell Signaling Technology (Danvers, MA 01923, United States); and GAPDH (1:5000, C1846) from Applygen (Beijing, China). Samples were treated with horseradish peroxidase-conjugated goat anti-mouse IgG or goat anti-rabbit IgG secondary antibodies (1:4,000, 31460, Thermo Fisher, Marietta, GA, 30006, United States) for 1 h at room temperature. Fusion FX (Vilber, France) and Enhanced Chemiluminescence kit (GE Healthcare, Chicago, Illinois, United States) were used to detect the signals. ImageJ software (National Institutes of Health, Bethesda, MD, United States) was used for quantitative Western blot analysis.



2.11 Statistical analysis

All cell experiments were performed at least three times, while all animal experiments were performed at least six times. GraphPad Prism software (version 8.0; GraphPad Software, La Jolla, United States) was used for statistical analysis. The measurement data are presented as the mean ± SEM, and statistical analyses were performed using one-way analysis of variance, followed by all pairwise multiple comparison procedures using the Bonferroni test. Categorical functional outcomes data, such as H&E staining, were expressed as quartiles, and the Mann-Whitney *U* test was used for group comparisons. Statistical significance was set at *p* < 0.05.

3 Results

3.1 H₂S inhibited myocardial disarray and fibrosis in UCM mice

To investigate the role of H₂S in UCM, we first examined CSE expression in the heart of each group of mice. Eight weeks after the operation, Western blotting results showed that the

expression of CSE protein in the heart of UCM mice was decreased compared with mice in the Sham group. Intraperitoneal injection of NaHS and L-Cys had no effect on the protein expression of CSE in the heart of UCM mice, but the expression of CSE was further decreased after PPG treatment (Figures 2E, F). Additionally, we measured the H₂S concentration in mouse plasma. Compared with mice in the Sham group, mice in the UCM group showed significantly lower H₂S levels. Intraperitoneal injection of NaHS and L-Cys reduced the decrease of H₂S levels, whereas PPG administration enhanced the decrease of H₂S levels in mice in the UCM group (Figure 2G).

Morphologically, H&E results suggested that compared with the mice in the Sham group, mice in the UCM group had obvious myocardial disorder (Figures 2A,C). In contrast, the above abnormalities could be reversed by NaHS and L-Cys treatment and further aggravated after PPG intraperitoneal injection (Figures 2A,C). Masson's staining also indicated that the level of cardiac fibrosis induced by 5/6 nephrectomy was significantly decreased when NaHS and L-Cys treatments were applied. However, the fibrosis level caused by 5/6 nephrectomy surgery in mice hearts was further aggravated after PPG treatment (Figures 2B,D).

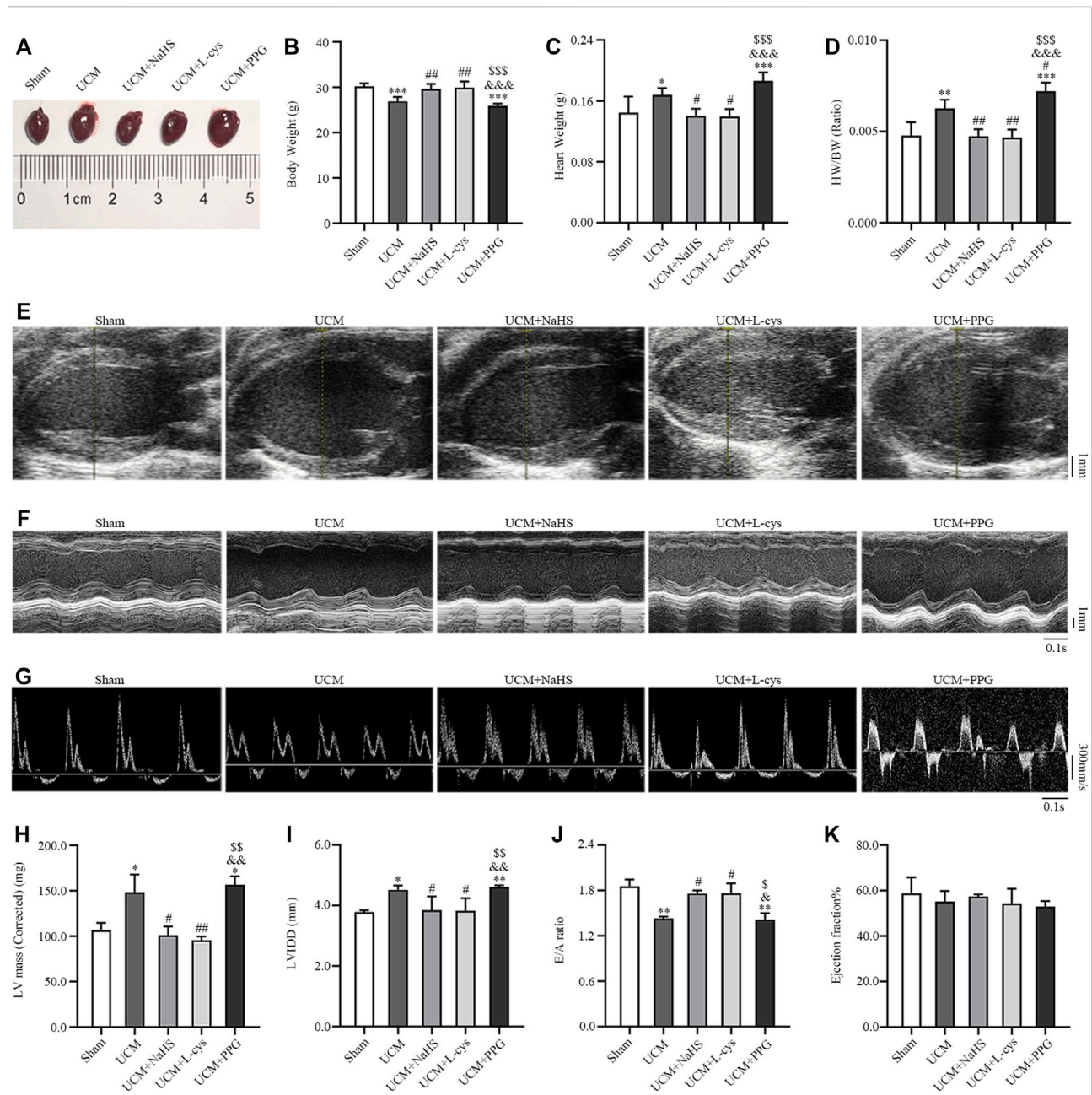
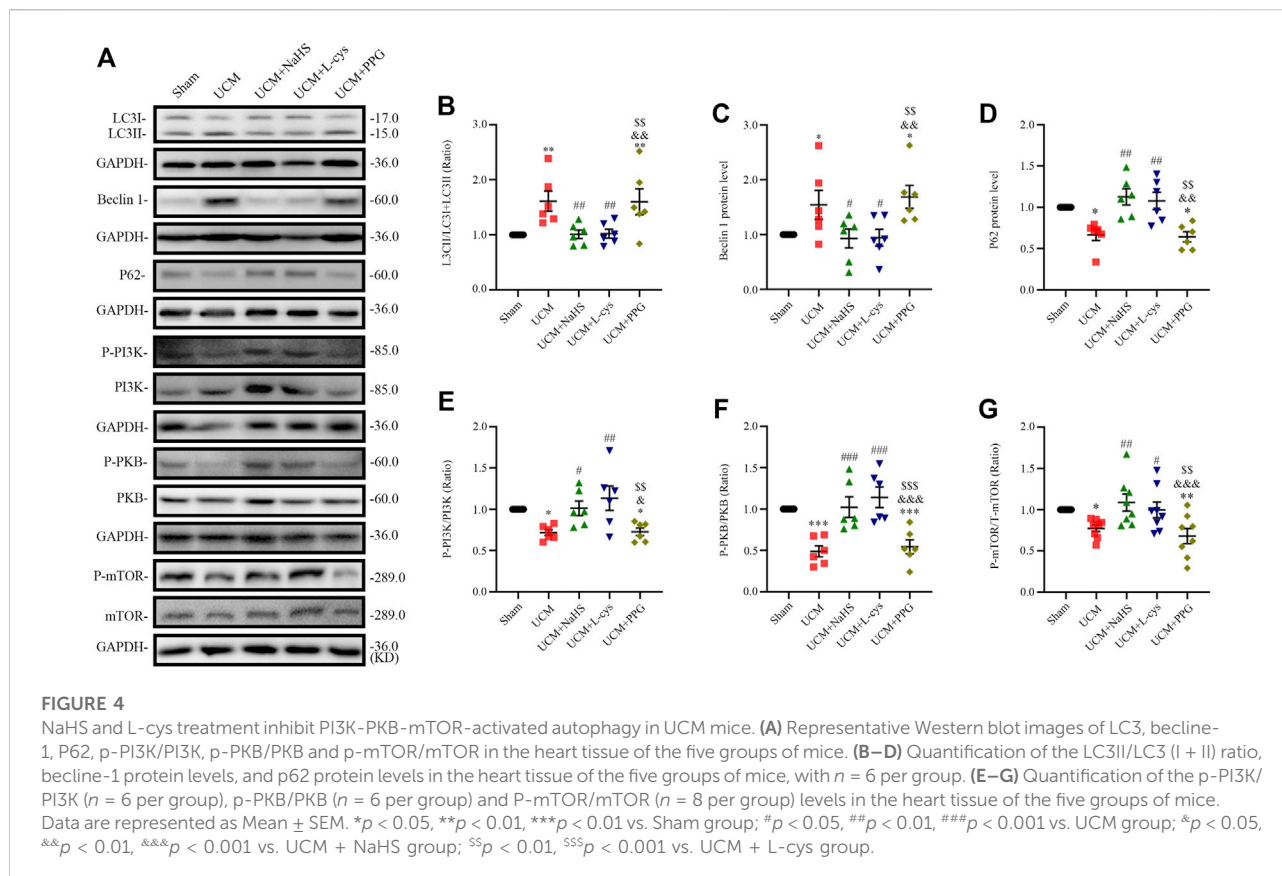


FIGURE 3

NaHS and L-cys treatment improved left ventricular hypertrophy (LVH) and diastolic dysfunction in UCM mice. (A) Representative images of heart tissues in the five groups of mice. (B–D) H₂S treatment reduces heart weight and heart weight/body weight. *n* = 6 per group. (E–G) Representative echocardiographic images in the five groups of mice. (E) Two-dimensional echocardiograms showing left ventricular long-axis views, with scale bar in mm on right. (F) M-mode echocardiograms showing left ventricular dimensions, with scale bar in mm on right and time stamp in seconds at the bottom. (G) Pulse-wave Doppler echocardiograms depicting mitral inflow velocities, with scale bar in mm on right and time stamp in seconds at bottom. (H–K) H₂S treatment improves LVH and diastolic dysfunction in UCM mice. *n* = 3 per group. E/A: the ratio of the early to late diastolic mitral inflow velocities; LVIDd: LV internal diameters at end-diastole; HW/BW: heart weight/body weight. Data are represented as Mean ± SEM. **p* < 0.05, ***p* < 0.01, ****p* < 0.001 vs Sham group; #*p* < 0.05, ##*p* < 0.01 vs. UCM group; &*p* < 0.05, &&*p* < 0.01, &&&*p* < 0.001 vs. UCM + NaHS group; \$*p* < 0.05, \$\$*p* < 0.01, \$\$\$*p* < 0.001 vs. UCM + L-cys group.



3.2 H₂S improved LVH and diastolic dysfunction in UCM mice

We investigated whether H₂S improves the prognosis of UCM *in vivo*. Compared with mice in the Sham group, the heart weight, heart weight/body weight (HW/BW), cardiac structural parameters LV mass and LVIdd were significantly higher, while body weight and diastolic functional values E/A were significantly lower in mice in the UCM group (Figures 3B–D, H–J). These abnormalities were largely reversed by NaHS and L-Cys treatment (Figures 3B–D, H–J). No significant differences were observed between groups for cardiac systolic ejection fractions (Figure 3K). Taken together, these studies identified that 5/6 nephrectomy-induced uremia can lead to cardiac dysfunction, including increased heart weight, LVH and diastolic dysfunction, which can be supplemented with H₂S torsion.

3.3 H₂S treatment inhibited PI3K-PKB-mTOR-activated autophagy in UCM mice

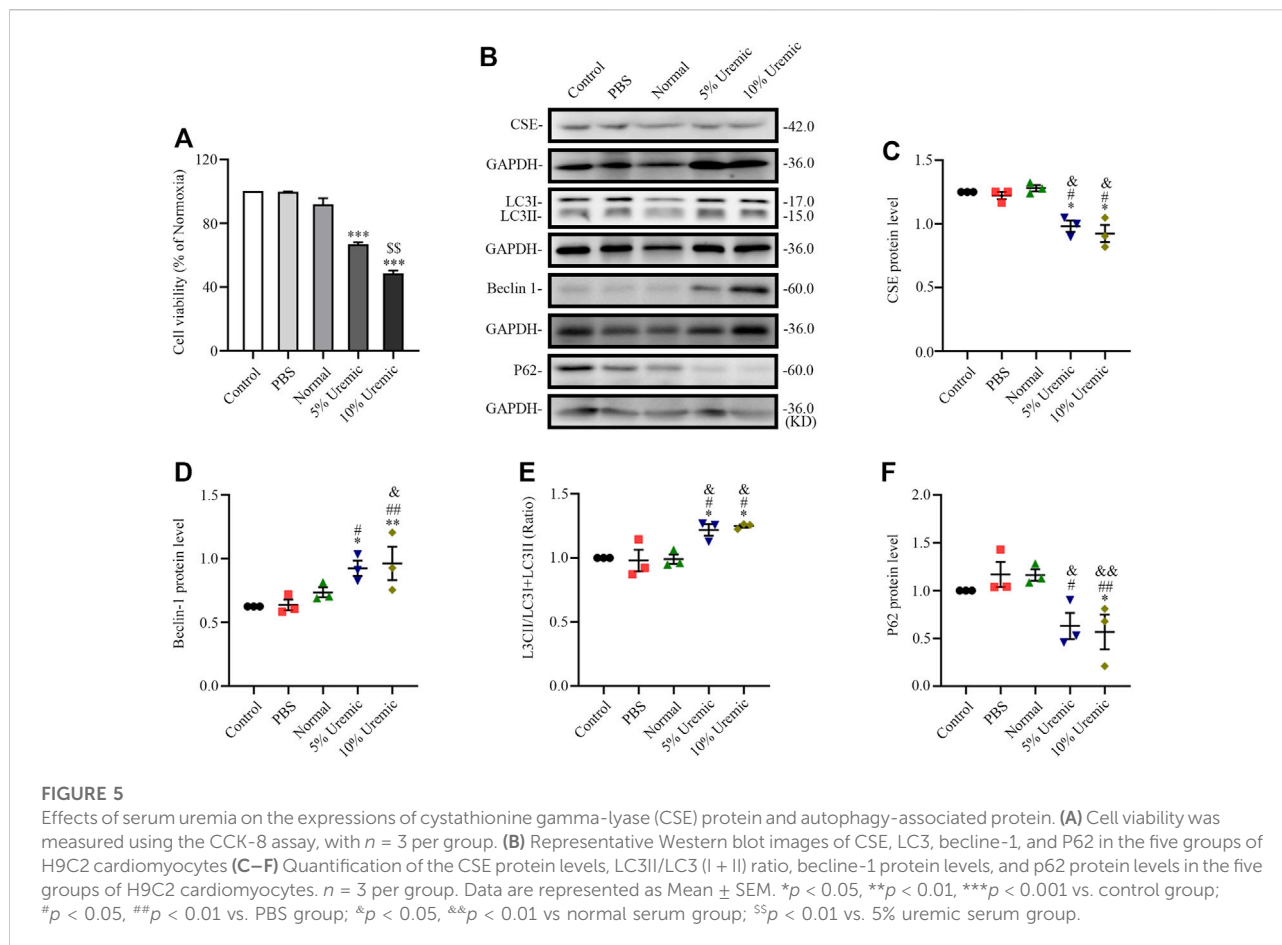
To determine whether 5/6 nephrectomy-induced UCM could regulate autophagy, we detected the expression of autophagy-related molecules in mouse heart tissue. We observed that the LC3II/LC3(I + II) ratio, beclin-1 protein levels, and p62 degradation significantly increased in UCM mice compared

to the Sham group (Figures 4A–D), suggesting that UCM may lead to overactive autophagy. However, intraperitoneal injection of NaHS and L-Cys decreased the LC3II/LC3 (I + II) ratio, beclin-1 protein levels, and p62 degradation. The same measures increased after PPG treatment, indicating that H₂S attenuated overactive autophagy in the heart tissue of 5/6 nephrectomy-induced UCM mice (Figures 4A–D).

Autophagy is mediated by several pathways, including the PI3K/PKB/mTOR pathway. We further verified the effects of H₂S on the PI3K-PKB-mTOR signaling pathway after 5/6 nephrectomy in mice. Western blotting analysis showed that protein expression levels of phosphorylated-PI3K (p-PI3K), p-PKB, and p-mTOR were significantly lower in the UCM and UCM + PPG groups, and we observed that the addition of NaHS and L-cys significantly increased the phosphorylation levels of PKB, PI3K, and mTOR (Figures 4A, E–G). These results suggest that H₂S inhibits excessive autophagy in the heart tissue by activating the PI3K-PKB-mTOR pathway.

3.4 Serum uremia induces overactive autophagy in H9C2 cardiomyocytes

The *in vitro* experiment was divided into four parts. In the first part, H9C2 cardiomyocytes were treated with normal serum and different concentrations of uremic serum, respectively. The results



showed that, following exposure to uremic serum for 24 h, the H9C2 cardiomyocytes showed significantly decreased viability and lower levels of CSE expression (Figures 5A–C). Western blotting showed the protein expression of LC3II/LC3(I + II) ratio, beclin-1 protein levels, and p62 degradation were higher in cardiomyocytes treated with uremic serum than in those treated with PBS or normal serum (Figures 5B, D–F). These results indicate that serum uremia may injure H9C2 cardiomyocytes *via* inducing overactive autophagy. In addition, H9C2 cells exposed to 10% uremic serum had higher cytotoxicity, beclin-1 protein levels and p62 degradation than those exposed to 5% uremic serum (Figures 5A–C, F). Thus, 10% uremic serum was selected to mimic the uremic environment *in vitro*.

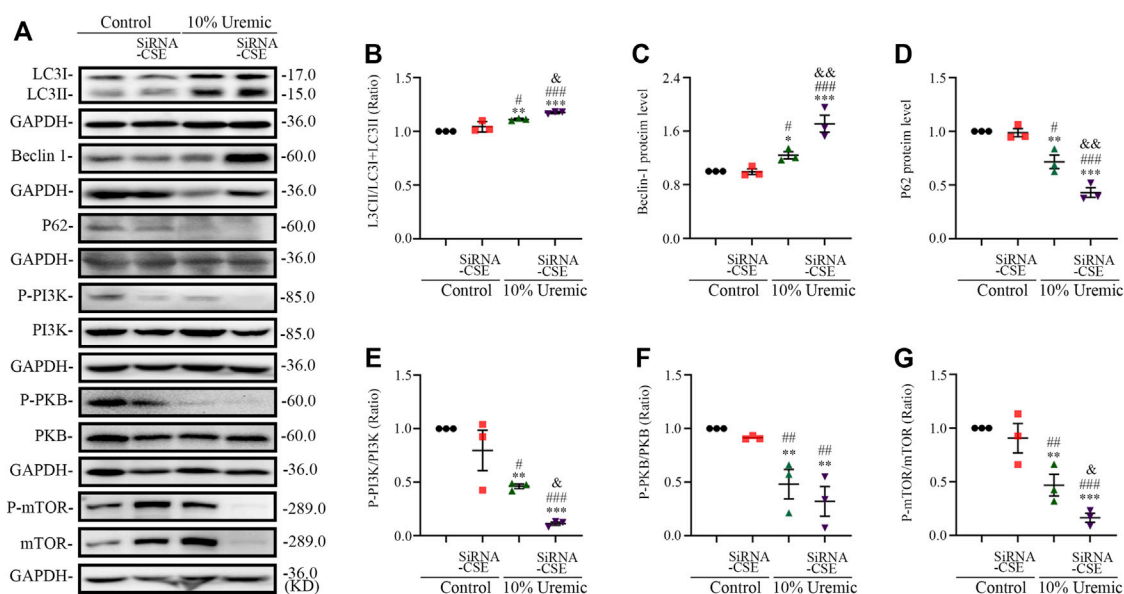
3.5 Endogenous H₂S deficiency exacerbates uremic serum-induced overactive autophagy in H9C2 cardiomyocytes

In the second phase of *in vitro* experiments, we attenuated the expression of CSE using siRNA transfection. The expression

levels of autophagy-related proteins (LC3-II, Beclin1, and p62) were quantified by Western blotting. We observed that the LC3II/LC3(I + II) ratio, beclin-1 protein levels, and p62 degradation significantly increased in the 10% uremic serum + SiRNA-CSE group, compared to the control and 10% uremic serum groups (Figures 6A–D). Western blot analysis showed that the protein expression levels of phosphorylated-PI3K (p-PI3K), phosphorylated-PKB (p-PKB), and p-mTOR were significantly lower in the 10% uremic toxin + SiRNA group than in the control and 10% uremic serum groups (Figures 6A, E–G). These results indicated that endogenous H₂S deficiency exacerbates excessive autophagy *via* the PI3K-PKB-mTOR pathway in H9C2 cardiomyocytes exposed to 10% uremic serum.

3.6 H₂S inhibited serum uremia-induced overactive autophagy in H9C2 cardiomyocytes

In the third phase of *in vitro* experiments, cardiomyocytes were treated with NaHS or PPG in 10% uremic serum. Cell

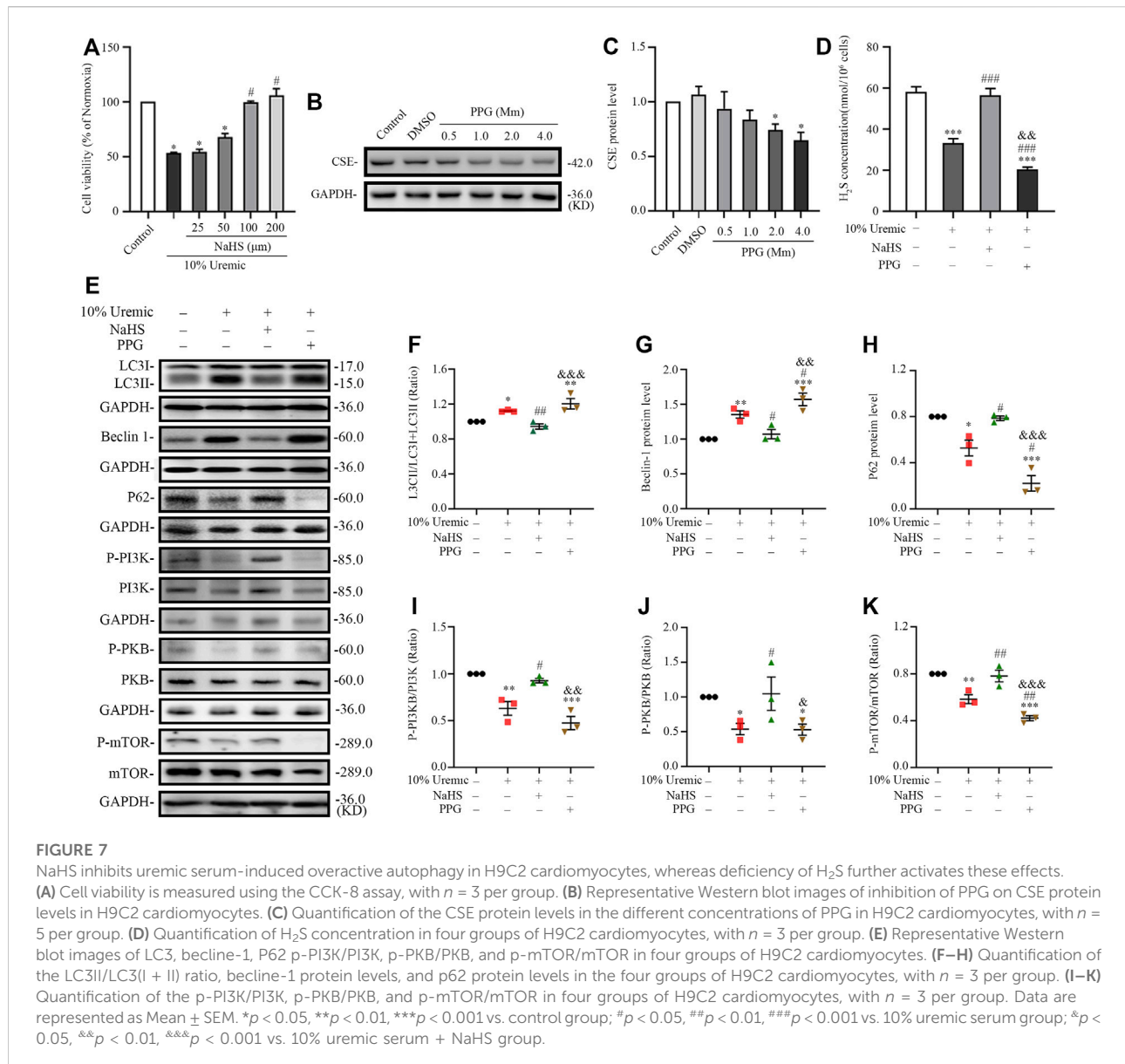


viability was measured using the CCK-8 assay. The expression levels of CSE and autophagy-related proteins (LC3-II, Beclin1, and p62) were quantified by Western blotting. The viability of H9C2 cardiomyocytes pretreated with 100 μ m NaHS for 30 min before exposure to serum uremia was significantly increased, indicating that NaHS can significantly reduce the cytotoxicity induced by serum uremia (Figure 7A). Thus, 100 μ m NaHS was selected for the pretreatment of cardiomyocytes exposed to 10% uremic toxin for 30 min. Western blotting showed that H9C2 cardiomyocytes treatment with 2.0 mm PPG for 24 h significantly attenuated the expression of CSE protein (Figures 7B,C). We further measured the H₂S concentration in H9C2 cardiomyocytes and found that the H₂S level significantly decreased in the 10% uremic serum group compared to the control group. Pre-treatment with NaHS increased the H₂S level, and the level decreased after treatment with 2.0 mm PPG for 24 h (Figure 7D). We observed that the LC3II/LC3(I + II) ratio, beclin-1 protein levels, and p62 degradation significantly increased in the 10% uremic serum group compared to the control group (Figures 7E–H). However, pre-treatment with NaHS decreased the LC3II/LC3 (I + II) ratio, beclin-1 protein levels, and p62 degradation, and increased after PPG treatment (Figures 7E–H). Western blot analysis showed that the protein expression levels of phosphorylated-PI3K (p-PI3K),

phosphorylated-PKB (p-PKB), and p-mTOR were significantly lower in the 10% uremic toxin group than in the control group (Figures 7D,I–K). We observed that pretreatment with NaHS significantly increased the phosphorylation levels of PKB, PI3K, and mTOR (Figures 7D,I–K). These results indicated that NaHS treatment suppressed excessive autophagy *via* the PI3K-PKB-mTOR pathway in H9C2 cardiomyocytes exposed to 10% uremic serum.

3.7 H₂S induces PKB and mTOR phosphorylation in H9C2 cardiomyocytes stimulated by serum uremia

In the fourth phase of *in vitro* experiments, H9C2 cardiomyocytes were treated with the PI3K inhibitor LY294002 prior to exposure to NaHS and 10% uremic serum, to investigate the role of the PI3K/PKB/mTOR pathway in the protective effects of H₂S. We observed that pretreatment with NaHS decreased the LC3II/LC3 (I + II) ratio, beclin-1 protein levels, and p62 degradation in 10% uremic serum. However, these protective effects of NaHS were blocked by LY294002 (Figures 8A–D). LY294002 also eliminated the stimulation of p-PKB and p-mTOR in the presence of NaHS but elicited no effect on the



expression levels of total PKB and mTOR (Figures 8A, E, F). These results further suggest that the PI3K/PKB/mTOR pathway is involved in the protective effects of H₂S.

These results suggest that H₂S increases the phosphorylation levels of PKB, PI3K, and mTOR and attenuates overactive autophagy in the hearts of UCM mice and serum uremia-treated cardiomyocytes. Inhibition of p-PI3K eliminated the protective effect of NaHS (Figure 9).

4 Discussion

UCM is a term used to describe patients with significant decline in renal function associated with cardiac structural and

functional changes, which is almost ubiquitous in patients with end-stage renal disease (Wang et al., 2017; Sodhi et al., 2020). UCM most commonly manifests as LVH with preserved ejection fraction and predisposes the heart to further cardiovascular complications in CKD (Bao et al., 2020). The severity and persistence of LVH in CKD patients are closely related to acute cardiovascular events (such as sudden cardiac death, arrhythmia and acute myocardial infarction) and death risk (Husain-Syed et al., 2015; Duni et al., 2017). The pathogenesis of uremic cardiomyopathy is multifactorial. The current treatment can improve the outcome, but not provide a cure (Lekawanvijit, 2018).

Autophagy is a key pathway of programmed cell death that helps maintain cardiac homeostasis at the basic level (Abdellatif et al., 2020). However, abnormal autophagy is associated with the development

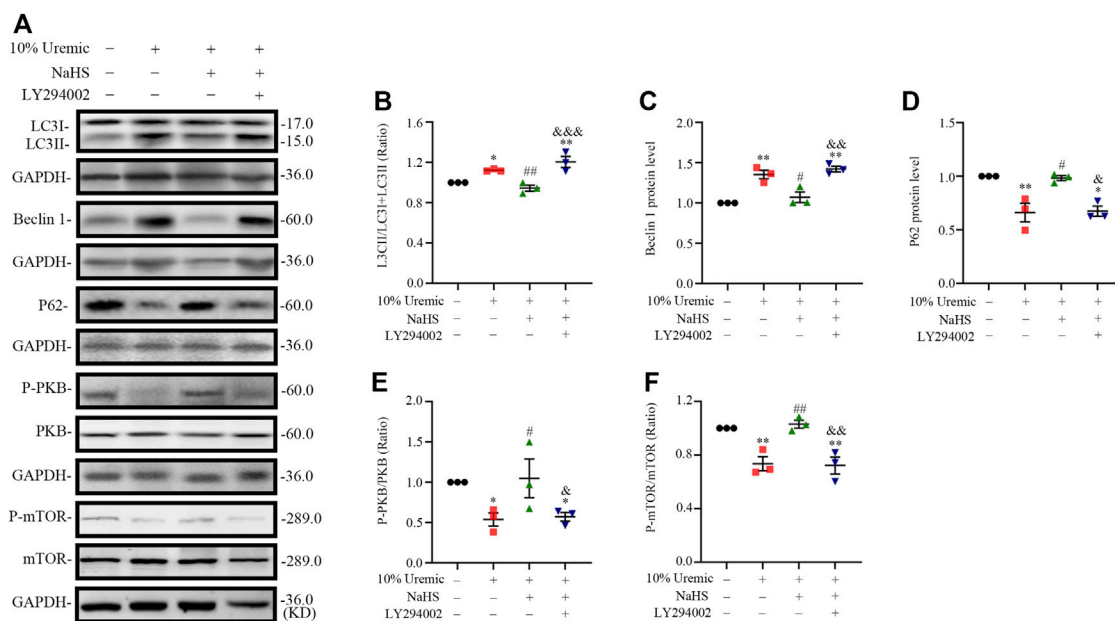


FIGURE 8

NaHS induces PKB and mTOR phosphorylation via PI3K/PKB pathway in H9C2 cardiomyocytes stimulated by uremic serum. (A) Representative Western blot images of LC3, beclin-1, P62, p-PKB/PKB and p-mTOR/mTOR in four groups of H9C2 cardiomyocytes. (B–D) Quantification of the LC3II/LC3 (I + II) ratio, beclin-1 protein levels, and p62 protein levels in the four groups of H9C2 cardiomyocytes, with $n = 3$ per group. (E,F) Quantification of the p-PKB/PKB and p-mTOR/mTOR in four groups of H9C2 cardiomyocytes, with $n = 3$ per group. Data are represented as Mean \pm SEM. * $p < 0.05$, ** $p < 0.01$ vs. control group; # $p < 0.05$, ## $p < 0.01$ vs. 10% serum uremia group; & $p < 0.05$, && $p < 0.01$, &&& $p < 0.001$ vs. 10% serum uremia + NaHS group.

and progression of heart disease (Shi et al., 2021). Some studies have shown that autophagy is generally decreased in aging hearts, and murine autophagy loss-of-function models develop exacerbated cardiac dysfunction (Shirakabe et al., 2016). While other studies have demonstrated that activation of autophagy has adverse effects on the heart, such as reperfusion injury, doxorubicin cardiomyopathy, and diabetic cardiomyopathy (Bartlett et al., 2017; Du et al., 2020; Zhang M. et al., 2021). Mialet-Perez et al. found that overactive autophagy promotes myocardial apoptosis and fibrosis and induces the transition from myocardial hypertrophy to heart failure (Mialet-Perez and Vindis, 2017). These inconsistent conclusions might be due to the different models used. Thus, there is an urgent need to understand the molecular mechanisms of UCM and identify drugs that are effective in treating UCM. In 5/6 nephrectomy mice, electrocardiogram showed that UCM developed cardiac alterations similar to those in patients with CKD-induced HFpEF. H&E and Masson's staining indicated that mice in the UCM group exhibited significant myocardial disarray and fibrosis, respectively. Western blotting demonstrated elevated levels of autophagy-associated proteins in mice in the UCM group. We also found that serum uremia increased the expression of autophagy-associated proteins *in vitro*. These results suggest that activation of autophagy aggravates heart injury in 5/6 nephrectomy mice.

H₂S is a newly discovered third gas signaling molecule after nitric oxide and carbon monoxide and has many biological

effects in the cardiovascular system (Luo et al., 2020). Cystathionine β -synthase (CBS), CSE, and 3-mercaptopyruvate sulfurtransferase (3-MST) are the three key enzymes for the production of H₂S in mammals (Bhatia and Gaddam, 2021). CSE is the major H₂S-producing enzyme in the cardiovascular system and has recently been shown to be expressed in the liver, lungs, and kidneys (Wang, 2012). The present study demonstrated that CSE protein levels are decreased in the HFpEF phase of UCM in mice, and intraperitoneal injection of PPG resulted in a further decrease. We also found that intraperitoneal injection of NaHS and L-Cys markedly ameliorated myocardial disarray and fibrosis levels, LVH, and dysfunction of UCM in mice; however, intraperitoneal injection of PPG aggravated these injuries. These results indicate that endogenous H₂S reduction and exogenous H₂S supplementation can inhibit UCM development. Subsequently, *in vitro*, we found that NaHS pretreatment attenuated the serum uremia-induced decrease in cardiomyocyte viability. We attenuated the expression of CSE using siRNA transfection and found endogenous H₂S deficiency exacerbates excessive autophagy. Thus, these data showed that H₂S could alleviate the development of UCM *in vivo* and *in vitro*. Furthermore, we found, by examining autophagy marker proteins (Beclin-1, LC3-II, and beclin-1) in the hearts of mice that underwent 5/6 nephrectomy and serum uremia-treated H9C2 cardiomyocytes, that supplementation with NaHS or

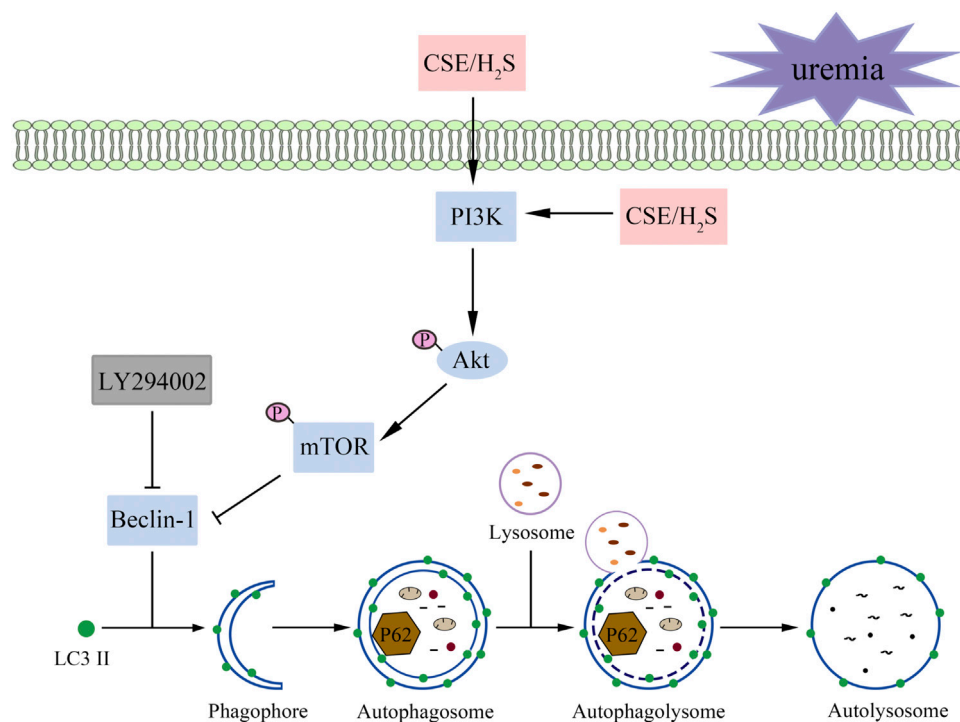


FIGURE 9

A proposed model illustrating the therapeutic effect of H₂S on UCM. Uremia inhibits the phosphorylation of PI3K in the heart and results in the heart dysfunction of UCM mice, while H₂S increases the phosphorylation levels of PKB, PI3K, and mTOR and attenuates overactive autophagy. In summary, H₂S alleviates uremic cardiomyopathy by regulating PI3K/PKB/mTOR-mediated autophagy in 5/6 nephrectomy mice.

L-Cys could decrease excessive autophagy activity. Consequently, we supposed that the protective effect of H₂S on UCM was achieved by downregulating autophagy activation.

There are various signaling pathways regulating autophagy, PI3K/PKB pathway is one of the classical pathways regulating autophagy (Shao et al., 2016). The PI3K/PKB pathway plays an essential role in regulating cell growth and survival, and some studies have shown that this pathway can also mediate the survival of myocardial cell in many situations (Wang et al., 2015). Furthermore, mTOR can be phosphorylated as a downstream target of PI3K/PKB pathway (Shao et al., 2016). Previous studies have shown that mTOR activation is closely related to autophagy, and its activation may inhibit autophagy activity (Ahumada-Castro et al., 2019). Nie et al. demonstrated that H₂S intervention in myocardial fibrosis is related to the inhibition of autophagy overactivation by upregulating of the PI3K/PKB/mTOR signal pathway (Nie et al., 2021). Xu et al. found that NaHS restores mitochondrial function and inhibits autophagy by activating the PI3K/PKB/mTOR signaling pathway to improve functional recovery after traumatic brain injury (Xu et al., 2018). The present study supports these previous findings, by demonstrating that supplementation with NaHS or L-Cys significantly increased the phosphorylation level of PI3K, PKB, and mTOR and decreased the autophagy-related protein

expression levels (Beclin-1, LC3II). LY294002, as a PI3K specific inhibitor, significantly reversed the effects of NaHS in serum uremia-treated H9C2 cardiomyocytes. These results suggest that H₂S may play a protective role in UCM by activating PI3K/PKB/mTOR pathway to inhibit excessive autophagy.

This study has several limitations. First, we did not use gene knockout or transgenic mice, but used pharmacological agonists or inhibitors which were selective. Second, we did not explore the dose gradient of L-Cys and NaHS injected intraperitoneally, but determined dose of the pharmacological agents from previous studies. Different doses may lead to different results, and future research should focus on addressing these important issues.

5 Conclusion

In summary, our study demonstrated for the first time that H₂S has protective effects in UCM, which might be explained by the inhibition of autophagy *via* the activation of the PI3K/PKB/mTOR signaling pathway. These results support the view that H₂S may be a potential therapeutic molecule to treat or prevent the development of UCM. It also increases the possibility of H₂S as an anti-UCM drug for clinical use.

Data availability statement

The original contributions presented in the study are included in the article/Supplementary Material, further inquiries can be directed to the corresponding author.

Ethics statement

The studies involving human participants were reviewed and approved by the Beijing Chao-Yang Hospital, Capital Medical University. The patients/participants provided their written informed consent to participate in this study. The animal study was reviewed and approved by Beijing Chao-Yang Hospital, Capital Medical University.

Written informed consent was obtained from the individual(s) for the publication of any potentially identifiable images or data included in this article.

Author contributions

HL and JF conceived and designed the experiment. HL, SW, and JF collected the samples, performed the experiments, and analyzed the corresponding results. HL and JF wrote the

References

- Abdellatif, M., Ljubojevic-Holzer, S., Madeo, F., and Sedej, S. (2020). Autophagy in cardiovascular health and disease. *Prog. Mol. Biol. Transl. Sci.* 172, 87–106. doi:10.1016/bs.pmbts.2020.04.022
- Ahumada-Castro, U., Silva-Pavez, E., Lovy, A., Pardo, E., Molgö, J., and Cárdenas, C. (2019). MTOR-Independent autophagy induced by interrupted endoplasmic reticulum-mitochondrial Ca (2+) communication: A dead end in cancer cells. *Autophagy* 15 (2), 358–361. doi:10.1080/15548627.2018.1537769
- Amador-Martínez, I., García-Ballhaus, J., Buelna-Chontal, M., Cortés-González, C., Massó, F., Jaisser, F., et al. (2021). Early inflammatory changes and CC chemokine ligand-8 upregulation in the heart contribute to uremic cardiomyopathy. *FASEB J.* 35 (8), e21761. doi:10.1096/fj.202100746R
- Bao, J. F., Hu, P. P., She, Q. Y., and Li, A. (2020). A land of controversy: Fibroblast growth factor-23 and uremic cardiac hypertrophy. *J. Am. Soc. Nephrol.* 31 (7), 1423–1434. doi:10.1681/asn.2020010081
- Bartlett, J. J., Trivedi, P. C., and Pulinkunnil, T. (2017). Autophagic dysregulation in doxorubicin cardiomyopathy. *J. Mol. Cell. Cardiol.* 104, 1–8. doi:10.1016/j.yjmcc.2017.01.007
- Bhatia, M., and Gaddam, R. R. (2021). Hydrogen sulfide in inflammation: A novel mediator and therapeutic target. *Antioxid. Redox Signal.* 34 (17), 1368–1377. doi:10.1089/ars.2020.8211
- Cheng, C. I., Lee, Y. H., Chen, P. H., Lin, Y. C., Chou, M. H., and Kao, Y. H. (2017). Cobalt chloride induces RhoA/ROCK activation and remodeling effect in H9c2 cardiomyoblasts: Involvement of PI3K/Akt and MAPK pathways. *Cell. Signal.* 36, 25–33. doi:10.1016/j.cellsig.2017.04.013
- Du, J., Li, Y., and Zhao, W. (2020). Autophagy and myocardial ischemia. *Adv. Exp. Med. Biol.* 1207, 217–222. doi:10.1007/978-981-15-4272-5_15
- Duni, A., Liakopoulos, V., Rapsomanikis, K. P., and Dounousi, E. (2017). Chronic kidney disease and disproportionately increased cardiovascular damage: Does oxidative stress explain the burden? *Oxid. Med. Cell. Longev.* 2017, 9036450. doi:10.1155/2017/9036450
- Hung, S. C., Kuo, K. L., Wu, C. C., and Tarng, D. C. (2017). Indoxyl sulfate: A novel cardiovascular risk factor in chronic kidney disease. *J. Am. Heart Assoc.* 6 (2), e005022. doi:10.1161/jaha.116.005022
- Husain-Syed, F., McCullough, P. A., Birk, H. W., Renker, M., Brocca, A., Seeger, W., et al. (2015). Cardio-pulmonary-renal interactions: A multidisciplinary approach. *J. Am. Coll. Cardiol.* 65 (22), 2433–2448. doi:10.1016/j.jacc.2015.04.024
- Kishore, R., Krishnamurthy, P., Garikipati, V. N., Benedict, C., Nickoloff, E., Khan, M., et al. (2015). Interleukin-10 inhibits chronic angiotensin II-induced pathological autophagy. *J. Mol. Cell. Cardiol.* 89, 203–213. doi:10.1016/j.yjmcc.2015.11.004
- Kolluru, G. K., Bir, S. C., Yuan, S., Shen, X., Pardue, S., Wang, R., et al. (2015). Cystathionine γ -lyase regulates arteriogenesis through NO-dependent monocyte recruitment. *Cardiovasc. Res.* 107 (4), 590–600. doi:10.1093/cvr/cvv198
- LaPenna, K. B., Polhemus, D. J., Doiron, J. E., Hidalgo, H. A., Li, Z., and Lefer, D. J. (2021). Hydrogen sulfide as a potential therapy for heart failure-past, present, and future. *Antioxidants (Basel)* 10 (3), 485. doi:10.3390/antiox10030485
- Leelahavanichkul, A., Yan, Q., Hu, X., Eisner, C., Huang, Y., Chen, R., et al. (2010). Angiotensin II overcomes strain-dependent resistance of rapid CKD progression in a new remnant kidney mouse model. *Kidney Int.* 78 (11), 1136–1153. doi:10.1038/ki.2010.287
- Lekawanvijit, S. (2018). Cardiotoxicity of uremic toxins: A driver of cardiorenal syndrome. *Toxins (Basel)* 10 (9), 352. doi:10.3390/toxins10090352
- Luo, W., Gui, D. D., Yan, B. J., Ren, Z., Peng, L. J., Wei, D. H., et al. (2020). Hydrogen sulfide switch phenomenon regulating autophagy in cardiovascular diseases. *Cardiovasc. Drugs Ther.* 34 (1), 113–121. doi:10.1007/s10557-019-06927-4
- Mei, Y., Thompson, M. D., Cohen, R. A., and Tong, X. (2015). Autophagy and oxidative stress in cardiovascular diseases. *Biochim. Biophys. Acta* 1852 (2), 243–251. doi:10.1016/j.bbadis.2014.05.005
- Memmos, E., and Papagianni, A. (2021). New insights into the role of FGF-23 and Klotho in cardiovascular disease in chronic kidney disease patients. *Curr. Vasc. Pharmacol.* 19 (1), 55–62. doi:10.2174/1570161118666200420102100
- Mialet-Perez, J., and Vindis, C. (2017). Autophagy in health and disease: Focus on the cardiovascular system. *Essays Biochem.* 61 (6), 721–732. doi:10.1042/ebc20170022

manuscript. All authors have read and approved the final manuscript.

Conflict of interest

The authors declare that the research was conducted in the absence of any commercial or financial relationships that could be construed as a potential conflict of interest.

Publisher's note

All claims expressed in this article are solely those of the authors and do not necessarily represent those of their affiliated organizations, or those of the publisher, the editors and the reviewers. Any product that may be evaluated in this article, or claim that may be made by its manufacturer, is not guaranteed or endorsed by the publisher.

Supplementary material

The Supplementary Material for this article can be found online at: <https://www.frontiersin.org/articles/10.3389/fphar.2022.1027597/full#supplementary-material>

- Nie, L., Liu, M., Chen, J., Wu, Q., Li, Y., Yi, J., et al. (2021). Hydrogen sulfide ameliorates doxorubicin-induced myocardial fibrosis in rats via the PI3K/AKT/mTOR pathway. *Mol. Med. Rep.* 23 (4), 299. doi:10.3892/mmr.2021.11938
- Porrello, E. R., and Delbridge, L. M. (2009). Cardiomyocyte autophagy is regulated by angiotensin II type 1 and type 2 receptors. *Autophagy* 5 (8), 1215–1216. doi:10.4161/auto.5.8.10153
- Powers, S. K., Morton, A. B., Ahn, B., and Smuder, A. J. (2016). Redox control of skeletal muscle atrophy. *Free Radic. Biol. Med.* 98, 208–217. doi:10.1016/j.freeradbiomed.2016.02.021
- Sárközy, M., Kovács, Z. Z. A., Kovács, M. G., Gáspár, R., Szűcs, G., and Dux, L. (2018). Mechanisms and modulation of oxidative/nitrative stress in type 4 cardio-renal syndrome and renal sarcopenia. *Front. Physiol.* 9, 1648. doi:10.3389/fphys.2018.01648
- Sciarretta, S., Maejima, Y., Zablocki, D., and Sadoshima, J. (2018). The role of autophagy in the heart. *Annu. Rev. Physiol.* 80, 1–26. doi:10.1146/annurev-physiol-021317-121427
- Shao, X., Lai, D., Zhang, L., and Xu, H. (2016). Induction of autophagy and apoptosis via PI3K/AKT/TOR pathways by azadirachtin A in *Spodoptera litura* cells. *Sci. Rep.* 6, 35482. doi:10.1038/srep35482
- Shi, M., Shepard, S., Zhou, Z., Maique, J., Seli, O., Moe, O. W., et al. (2021). High dietary phosphate exacerbates and acts independently of low autophagy activity in pathological cardiac remodeling and dysfunction. *Cells* 10 (4), 777. doi:10.3390/cells10040777
- Shirakabe, A., Ikeda, Y., Sciarretta, S., Zablocki, D. K., and Sadoshima, J. (2016). Aging and autophagy in the heart. *Circ. Res.* 118 (10), 1563–1576. doi:10.1161/circresaha.116.307474
- Sodhi, K., Wang, X., Chaudhry, M. A., Lakhani, H. V., Zehra, M., Pratt, R., et al. (2020). Central role for adipocyte Na₂K-ATPase oxidant amplification loop in the pathogenesis of experimental uremic cardiomyopathy. *J. Am. Soc. Nephrol.* 31 (8), 1746–1760. doi:10.1681/asn.2019101070
- Spoto, B., Pisano, A., and Zoccali, C. (2016). Insulin resistance in chronic kidney disease: A systematic review. *Am. J. Physiol. Ren. Physiol.* 311 (6), F1087–F1108. doi:10.1152/ajprenal.00340.2016
- Vanholder, R., Schepers, E., Pletinck, A., Nagler, E. V., and Glorieux, G. (2014). The uremic toxicity of indoxyl sulfate and p-cresyl sulfate: A systematic review. *J. Am. Soc. Nephrol.* 25 (9), 1897–1907. doi:10.1681/asn.2013101062
- Wang, R. (2012). Physiological implications of hydrogen sulfide: A whiff exploration that blossomed. *Physiol. Rev.* 92 (2), 791–896. doi:10.1152/physrev.00017.2011
- Wang, X., Liu, J., Drummond, C. A., and Shapiro, J. I. (2017). Sodium potassium adenosine triphosphatase (Na/K-ATPase) as a therapeutic target for uremic cardiomyopathy. *Expert Opin. Ther. Targets* 21 (5), 531–541. doi:10.1080/14728222.2017.1311864
- Wang, X., and Shapiro, J. I. (2019). Evolving concepts in the pathogenesis of uremic cardiomyopathy. *Nat. Rev. Nephrol.* 15 (3), 159–175. doi:10.1038/s41581-018-0101-8
- Wang, Z. G., Wang, Y., Huang, Y., Lu, Q., Zheng, L., Hu, D., et al. (2015). bFGF regulates autophagy and ubiquitinated protein accumulation induced by myocardial ischemia/reperfusion via the activation of the PI3K/Akt/mTOR pathway. *Sci. Rep.* 5, 9287. doi:10.1038/srep09287
- Wu, H., Ye, M., Liu, D., Yang, J., Ding, J. W., Zhang, J., et al. (2019). UCP2 protect the heart from myocardial ischemia/reperfusion injury via induction of mitochondrial autophagy. *J. Cell. Biochem.* 120 (9), 15455–15466. doi:10.1002/jcb.28812
- Xiao, T., Luo, J., Wu, Z., Li, F., Zeng, O., and Yang, J. (2016). Effects of hydrogen sulfide on myocardial fibrosis and PI3K/AKT1-regulated autophagy in diabetic rats. *Mol. Med. Rep.* 13 (2), 1765–1773. doi:10.3892/mmr.2015.4689
- Xu, K., Wu, F., Xu, K., Li, Z., Wei, X., Lu, Q., et al. (2018). NaHS restores mitochondrial function and inhibits autophagy by activating the PI3K/Akt/mTOR signalling pathway to improve functional recovery after traumatic brain injury. *Chem. Biol. Interact.* 286, 96–105. doi:10.1016/j.cbi.2018.02.028
- Zhang, M., Sui, W., Xing, Y., Cheng, J., Cheng, C., Xue, F., et al. (2021a). Angiotensin IV attenuates diabetic cardiomyopathy via suppressing FoxO1-induced excessive autophagy, apoptosis and fibrosis. *Theranostics* 11 (18), 8624–8639. doi:10.7150/thno.48561
- Zhang, Q. Y., Jin, H. F., Chen, S., Chen, Q. H., Tang, C. S., Du, J. B., et al. (2018). Hydrogen sulfide regulating myocardial structure and function by targeting cardiomyocyte autophagy. *Chin. Med. J.* 131 (7), 839–844. doi:10.4103/0366-6999.228249
- Zhang, T. Y., Zhao, B. J., Wang, T., and Wang, J. (2021b). Effect of aging and sex on cardiovascular structure and function in wildtype mice assessed with echocardiography. *Sci. Rep.* 11 (1), 22800. doi:10.1038/s41598-021-02196-0
- Zhou, X., An, G., and Chen, J. (2014). Hydrogen sulfide improves left ventricular function in smoking rats via regulation of apoptosis and autophagy. *Apoptosis* 19 (6), 998–1005. doi:10.1007/s10495-014-0978-z